$NaFe_{0.56}Cu_{0.44}As$: A Pnictide Insulating Phase Induced by On-Site Coulomb Interaction

C. E. Matt,[1,2,*] N. Xu,[1,3] Baiqing Lv,[1,4] Junzhang Ma,[1,4] F. Bisti,[1] J. Park,[1] T. Shang,[1,3,5] Chongde Cao,[6,7] Yu Song,[6] Andriy H. Nevidomskyy,[6] Pengcheng Dai,[6] L. Patthey,[1] N. C. Plumb,[1] M. Radovic,[1] J. Mesot,[1,2,3] and M. Shi[1,†]

[1]*Swiss Light Source, Paul Scherrer Institut, CH-5232 Villigen PSI, Switzerland*

[2]*Laboratory for Solid State Physics, ETH Zürich, CH-8093 Zürich, Switzerland*

[3]*Institute of Condensed Matter Physics, École Polytechnique Fédérale de Lausanne, CH-10 15 Lausanne, Switzerland*

[4]*Beijing National Laboratory for Condensed Matter Physics and Institute of Physics, Chinese Academy of Sciences, Beijing 100190, China*

[5]*Laboratory for Developments and Methods, Paul Scherrer Institut, CH-5232 Villigen, Switzerland*

[6]*Department of Physics and Astronomy, Rice University, Houston, Texas 77005, USA*

[7]*Department of Applied Physics, Northwestern Polytechnical University, Xian 710072, China*

(Received 1 June 2016; revised manuscript received 4 August 2016; published 25 August 2016)

In the studies of iron pnictides, a key question is whether their bad-metal state from which the superconductivity emerges lies in close proximity with a magnetically ordered insulating phase. Recently, it was found that at low temperatures, the heavily Cu-doped $NaFe_{1-x}Cu_xAs$ ($x > 0.3$) iron pnictide is an insulator with long-range antiferromagnetic order, similar to the parent compound of cuprates but distinct from all other iron pnictides. Using angle-resolved photoemission spectroscopy, we determined the momentum-resolved electronic structure of $NaFe_{1-x}Cu_xAs$ ($x = 0.44$) and identified that its ground state is a narrow-gap insulator. Combining the experimental results with density functional theory (DFT) and DFT + U calculations, our analysis reveals that the on-site Coulombic (Hubbard) and Hund's coupling energies play crucial roles in the formation of the band gap about the chemical potential. We propose that at finite temperatures, charge carriers are thermally excited from the Cu-As-like valence band into the conduction band, which is of Fe 3d-like character. With increasing temperature, the number of electrons in the conduction band becomes larger and the hopping energy between Fe sites increases, and finally the long-range antiferromagnetic order is destroyed at $T > T_N$. Our study provides a basis for investigating the evolution of the electronic structure of a Mott insulator transforming into a bad metallic phase and eventually forming a superconducting state in iron pnictides.

DOI: 10.1103/PhysRevLett.117.097001

Similar to the cuprates and iron chalcogenides, in the phase diagram of the iron pnictides, a superconducting dome develops upon doping a nonsuperconducting, often magnetically ordered, parent compound. The superconducting dome and/or magnetic phase are formed from an underlying normal state which exhibits bad-metal behavior with large electrical resistivity at room temperature [1–4]. It has been proposed that the proximity to a Mott insulating phase is responsible for the bad-metal behavior and increase in the electronic correlations in those compounds [3,5]. In the studies of iron chalcogenides, it has also been suggested that the (orbital-dependent) Mott physics plays a key role in the mechanism for the insulating behavior. In cuprates, electron-electron correlations are reduced by doping either electrons or holes into the Mott insulating parent compound, with superconductivity occurring at a few percent of doping [6–8]. In contrast, correlation effects in the iron pnictides are only weakened with the electron doping but enhanced when doping holes into their parent compounds [9–12]. However, for all the iron pnictides, even up to the highest possible hole-doping level (e.g., fully replacing Ba with K in the widely studied $Ba_{1-x}K_xFe_2As_2$), an antiferromagnetically (AFM) ordered insulating state does not occur [11,13]. It would be highly interesting to identify and investigate an iron-pnictide family that undergoes an AFM insulating—(bad) metallic—superconducting phase transition tuned by doping and study these compounds' electronic structures in distinct phases.

Very recently, it has been shown that, adjacent to the superconducting phase, an AFM insulating state occurs in heavily doped $NaFe_{1-x}Cu_xAs$ [14,15]. For $x > 0.3$, below $T_N = 200$ K, the system develops antiferromagnetic order, which becomes long range for $x \geq 0.44$. The spin arrangement is depicted in Fig. 1(c), with a magnetic moment $\sim 1.1\mu_B$ per iron site, ten times larger than that in the parent compound NaFeAs [16]. Using angle-resolved photoemission spectroscopy (ARPES), combined with density functional theory (DFT) and DFT + U calculations, we reveal that in $NaFe_{1-x}Cu_xAs$ with high x values ($x = 0.44$), the Hubbard U and Hund's coupling J_H have a strong effect on the underlying electronic structure by opening a finite energy gap at the Fermi level (E_F). The ARPES results are significantly different from the electronic structure obtained from DFT calculations but can be reproduced by DFT + U calculations with the inclusion of U and J_H to account for the on-site Coulomb interaction. We show that the main effect of the interactions is to shift the Fe d orbital-related bands to higher binding energies, which results in the ground state of $NaFe_{0.56}Cu_{0.44}As$ being an insulator.

High-quality single crystals of $NaFe_{1-x}Cu_xAs$ were grown using the self-flux method as described in Ref. [15].

ARPES experiments were carried out at the Surface and Interface Spectroscopy beam line [20], Swiss Light Source, using a Scienta R4000 electron analyzer with total energy and angular resolutions of ~20 meV and ~0.15°, respectively. Samples were cleaved *in situ* under ultrahigh vacuum conditions ($<5 \times 10^{-11}$ mbar). The DFT calculations were performed using the WIEN2K package [21] with the crystal structure shown in Fig. 1(a) and the lattice parameters ($a = b = 5.72$ Å, $c = 13.85$ Å) determined from neutron diffraction on $NaFe_{0.56}Cu_{0.44}As$ [14] and with interaction parameters $U = 3.15$ eV and $J_H = 0.4$ eV as calculated for LiFeAs [22,23].

To get more insight into the insulating behavior of $NaFe_{0.56}Cu_{0.44}As$ at low temperatures as observed in the transport measurements [Fig. 1(b) and Refs. [14,15]], we have performed electronic structure calculations without and with on-site correlations by using DFT and DFT + U methods, respectively. The DFT calculation predicts a semimetallic state with an electronlike pocket at Γ (Fe character) and a holelike pocket around M (Cu-As character); see Fig. 1(d). These pockets produce a finite density of states at E_F (Fig. S1), which is inconsistent with the insulating behavior of $NaFe_{0.56}Cu_{0.44}As$. On the other hand, if U and J_H are included in the calculations (DFT + U), the valence bands get pushed to higher binding energies and the conduction bands are shifted up, resulting in a finite energy gap between valence and conduction bands [Figs. 1(e) and 1(f)]. The magnitude of the band shift depends strongly on the elemental and orbital composition of the bands; it is negligible for the Cu- and As-derived bands but large for the bands formed by Fe d orbitals. Among the Fe d orbitals, the on-site Coulomb interaction has the strongest effect on d_{xy}- and d_{z2}-orbital dominated energy bands. Similar to the case of $BaCu_2As_2$ [37,38], the DFT band near E_F around the M point is formed by the hybridization of As $4p$ and Cu $3d$ orbitals with Fe $3d$ orbitals [23]. The inclusion of on-site Coulomb interaction lifts the hybridization, pushing the Cu-As band below E_F and shifting the Fe band above E_F.

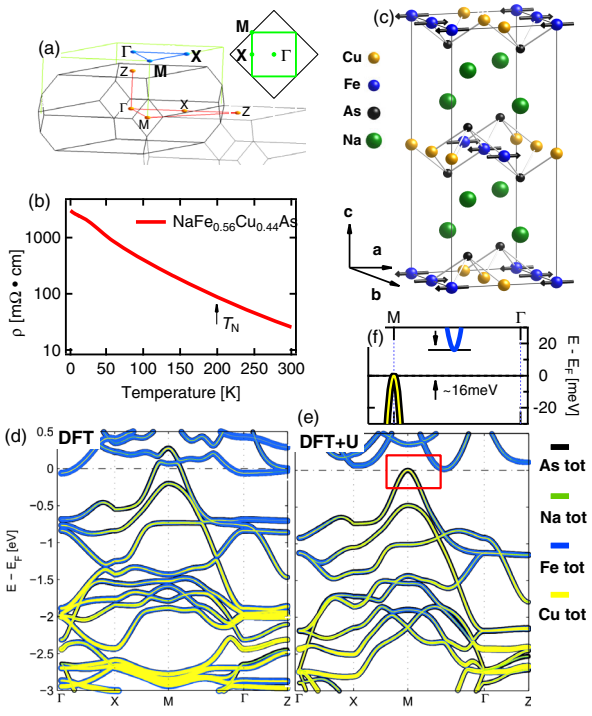

FIG. 1. Electronic structure of $NaFe_{0.5}Cu_{0.5}As$ calculated by DFT and DFT + U. (a) BZ with high symmetry points and lines indicated. The light green line indicates the projected BZ. Inset: Light green lines denote the projected BZ of $NaFe_{0.56}Cu_{0.44}As$, black lines the BZ of the two-Fe unit cell of $BaFe_2As_2$ as defined in Refs. [17,18]. (b) Temperature dependence of the in-plane resistivity for $NaFe_{0.56}Cu_{0.44}As$. The arrow indicates T_N as obtained from neutron diffraction [14]. (c) The crystal structure [19]. (d),(e) The band structure along high symmetry lines from DFT and DFT + U calculations, respectively. (f) Zoom-in of the red box in (e), showing the band gap about E_F.

Figure 2 shows ARPES spectra and their curvature plots along the high symmetry lines in the Brillouin zone (BZ). The overlaid lines are the calculated band dispersion. The overall agreement between the ARPES spectra and the calculated DFT + U electronic structure is significant. (1) No electronlike pocket around the Γ point was observed near E_F, which is consistent with the predication of DFT + U calculations and different from that of DFT. (2) Moving from the Γ or X point to the M point, the band approaches but does not cross the Fermi level; thus, no holelike pocket around the M point is formed. (3) At high binding energies, the ARPES results agree better with DFT + U than with DFT. For example, the multiple flat Fe/Cu-derived bands at E-$E_F \sim -3$ eV in the DFT calculations were not observed by ARPES [Fig. 2(c1)]. We would like to point out that in contrast to the DFT calculations on the majority of iron pnictides, no shift of individual bands is required in order to match the ARPES results. Our ARPES results reveal that the ground state of $NaFe_{0.56}Cu_{0.44}As$ is an insulator, consistent with the scanning tunneling microscopy (STM) study of heavily Cu-doped $NaFe_{1-x}Cu_xAs$ ($x = 0.3$), which showed diminished density of states at the chemical potential [39]. In Figs. 2(d1) and 2(d2), we plot the ARPES spectra taken in the paramagnetic state at 260 K, well above $T_N \sim 200$ K; the dispersion is almost identical to that at low temperature (15 K). However, as shown in Fig. 2(e), the DFT + U calculation in the paramagnetic state predicts a large, holelike Fermi surface around M, which is not observed in the ARPES measurement. We would like to emphasize that the local magnetic moment on the Fe sites plays an essential role in order to explain the observed electronic structure below and above T_N.

To further explore the insulating behavior of $NaFe_{1-x}Cu_xAs$, we have carried out ARPES measurements in several Brillouin zones. Figure 3 shows ARPES intensity

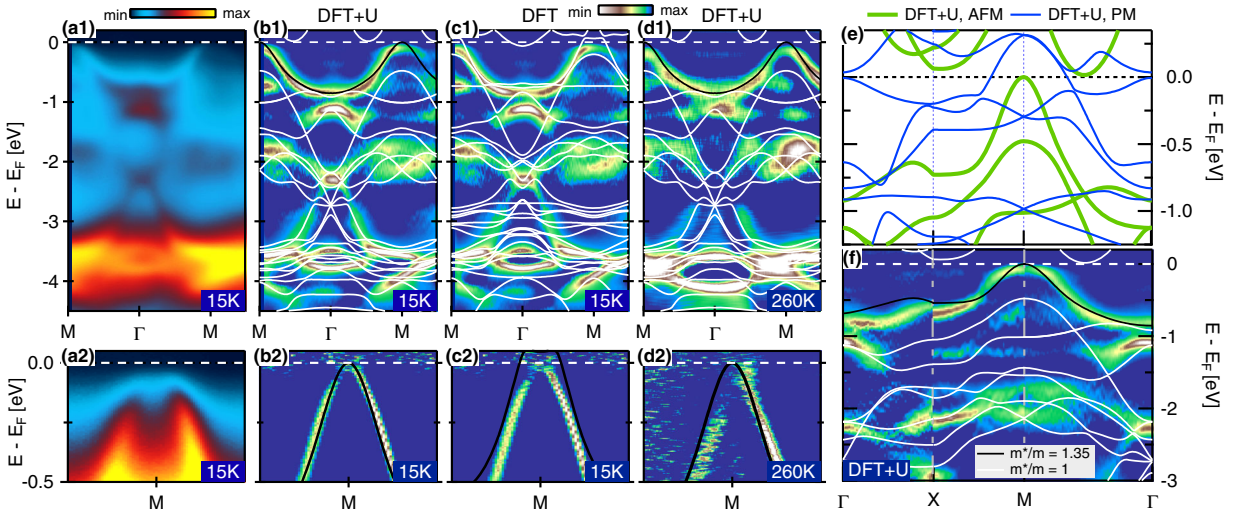

FIG. 2. ARPES spectra of $NaFe_{0.56}Cu_{0.44}As$. (a1),(a2) ARPES spectrum along the M-Γ-M direction, taken at $T = 15$ K with $hv = 52$ eV and circularly polarized photons in (b1) and (b2), respectively. (c1),(c2) Curvature plot of the ARPES spectra in (a1) and (a2), respectively. The superimposed lines are the band dispersion from DFT + U and DFT calculations, as indicated. The calculated dispersion drawn in black is renormalized by a factor of 1.35. White lines represent nonrenormalized bands. (d1),(d2) The same as (b1) and (b2), but the ARPES spectrum is obtained at $T = 260$ K. (e) Band dispersion as calculated by DFT + U for the AFM (green lines) and paramagnetic (PM) state (blue lines). (f) Curvature plot of the ARPES spectrum at $T = 15$ K along high symmetry lines as indicated in Fig. 1(a). The superimposed lines are the band dispersion from the DFT + U calculation.

maps at fixed binding energies. In Figs. 3(a) and 3(b), the intensity map obtained at 15 K is plotted 25 and 300 meV below E_F since the spectral intensity at E_F is vanishing. As expected, except for the (Cu, As)-formed valence band [Figs. 2(a1)–2(b2)] predicted by the DFT + U calculation, no other band appears at these two energies. The ARPES intensity maps at different binding energies vary little with k_z, indicating that the electronic structure of $NaFe_{0.56}Cu_{0.44}As$ is quasi-two-dimensional. These observations are in concert with DFT + U calculations and provide spectroscopic evidence that the system is insulating at low temperatures. In the DFT + U calculations, the effect of including U and J_H is to remove the hybridization of As p and Cu d with Fe 3d orbitals and push the bands dominated by Fe 3d orbitals away from the chemical potential. The remaining band near E_F is mainly composed by Cu orbitals [Fig. 1(e)]. It has been shown in Ref. [14] that the Cu is close to the d^{10} configuration. This

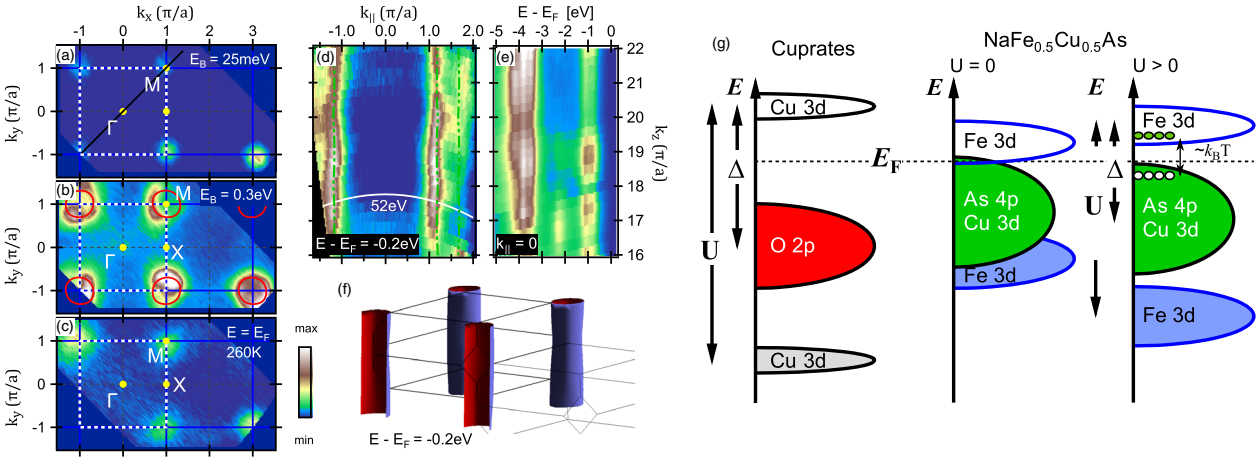

FIG. 3. (a),(b) ARPES intensity maps at energies E-$E_F = -25$ meV and E-$E_F = -300$ meV, respectively. The spectra were acquired with $hv = 52$ eV and circularly polarized photons at $T = 15$ K. The maps have been integrated over an energy window of ±10 meV. (c) ARPES intensity map at E_F, obtained at $T = 260$ K. Because of the thermal broadening, finite intensity appears at the E_F. (d) ARPES intensity map at energies E-$E_F = -200$ meV in the $k_\parallel - k_z$ plane, where $k_\parallel$ is along the Γ-M direction. (e) The dispersion along the k_z direction at $k_\parallel = 0$. (f) Sketch of the constant energy surface at E-$E_F = -200$ meV in the 3D BZ, calculated by DFT + U. (g) Schematic of the electronic structure of cuprate parent compounds and $NaFe_{0.56}Cu_{0.44}As$ for the noninteracting case ($U = 0$) and for the case of finite interactions. The quantity $\sim k_B T$ indicates the thermal excitations of electrons from the valence to conduction bands.

could explain why the valence band near E_F is only renormalized by a factor of ~1.35 [Figs. 2(b2) and 2(d2)], which is much smaller than the renormalization factor in the Fe-pnictide parent or hole-doped superconducting Fe-pnictide compounds (typically ~2–4), whose Fe 3d orbitals are partially filled [11,40–42].

In Fig. 3(c), we plot the ARPES intensity map at E_F at $T = 260$ K. Because of thermal broadening, we observe finite spectral weight around M, very similar to the intensity map taken at low temperatures, slightly below E_F [see Fig. 3(a)]. The primary results of our ARPES measurements are the observation of a valence band which is touching, but not crossing, the Fermi level and an unexpectedly temperature-independent overall band structure which remains unchanged far above T_N.

Having established that $NaFe_{0.56}Cu_{0.44}As$ is an insulator in the ground state due to correlation effects, we turn to the natural question of how the long-range AFM order disappears at temperatures above the Néel ordering temperature ($T_N \sim 200$ K), as observed in neutron diffraction measurements [14]. In Mott insulators, the AFM ordering of local magnetic moments is related to the superexchange energy, which is proportional to t^2/U, where t is the hopping integral that scales with the kinetic energy of charge carriers moving in solids [6,43,44]. If the on-site Coulomb repulsion exceeds the kinetic energy, the intersite hopping of charge carriers is blocked, causing them to become localized. On the other hand, if the Coulomb energy barrier can be overcome due to a large hopping energy, electrons or holes are delocalized and the long-range AFM ordering is suppressed. It is known that long-range AFM order in a Mott insulator can be suppressed by changing the band filling with chemical doping. For example, in cuprates, at low temperatures, long-range AFM order is destroyed by doping a few percent of holes or electrons into the Mott insulating parent compounds. Note that the Mott gap (or, more generally, charge-transfer gap) needs not be suppressed completely for the long-range AFM order to disappear: the insulating Mott state without long-range magnetic order often persists above the Néel temperature [45–48]. This consideration provides a possible explanation for the AFM ordering in $NaFe_{0.56}Cu_{0.44}As$ observed in neutron scattering experiments, as well as its temperature dependence. Figure 3(g) schematically depicts the density of states of $NaFe_{0.56}Cu_{0.44}As$ in comparison with the parent compounds of cuprates [49]. Because of the on-site Coulombic repulsion, the Fe d orbital-related conduction and valence bands move farther away from the chemical potential [Fig. 3(g)]. About E_F, a small indirect band gap occurs between the top of the valence band formed by (Cu, As) and the bottom of conduction bands dominated by Fe d states. In the ground state, the system is insulating: the virtual hopping of electrons with antiparallel spins from one Fe site to the next, restricted by the Pauli exclusion principle, leads to the formation of an AFM arrangement in the Fe lattice. Upon increasing temperature, due to the small band gap and thermal excitation, the lowest conduction band starts to be populated by electrons from the highest Cu-As valence band, which leaves holes in the valence band [see Fig. 3(g)]. Because the holes (electrons) in the valence (conduction) band are mobile, the resistivity of the material decreases, as manifested in transport measurements [see Fig. 1(b)], similarly to thermally activated transport in a narrow-band semiconductors. This hopping of the thermally excited electrons in the lowest conduction band [which has Fe 3d character; see Figs. 1(e) and 1(f)] suppresses the long-range AFM order in the Fe lattice, while the charge gap persists. This is consistent with the insulating behavior of resistivity observed well above the Néel temperature in $NaFe_{1-x}Cu_xAs$ [14,15]. Our ARPES results obtained at 260 K (well above T_N) show that the band dispersion as well as the band renormalization near E_F are very similar to that at 15 K (well below T_N), indicating that there is no significant change in the electronic structure as T_N is crossed. This would suggest that the disappearance of the long-range AFM ordering at $T > 200$ K is indeed related to the occupation of the lowest conduction and highest valence bands, without closing the Mott charge-transfer gap. The robustness of the electronic structure is consistent with transport measurements: upon increasing temperature, the resistivity smoothly decreases and the insulating behavior persists at least up to 300 K; no abnormal behavior is observed in the vicinity of T_N; see Fig. 1(b). While not excluding other more sophisticated models (e.g., orbital-selective Mott physics [9,10,50,51]) that would be able to quantitatively account for the experimental results on this material, the basic picture described here provides a qualitatively consistent explanation for the experimental results from neutron scattering, transport, and ARPES measurements. This picture in which Mott physics plays a key role for the insulating behavior in highly Cu-doped $NaFe_{1-x}Cu_xAs$ is strongly supported by a recent STM study on insulating $NaFe_{0.7}Cu_{0.3}As$, which reports striking similarities to lightly doped cuprates [39]. The early ARPES studies on $NaFe_{1-x}Cu_xAs$ with x up to 0.14 showed that, except for introducing extra charge carriers, the overall band dispersion barely changes with Cu doping, and the Fermi surface and/or all the energy bands near E_F are dominated by Fe 3d orbitals [52]. It is of high interest to reveal the momentum-resolved electronic structure with ARPES in order to get further insight into the evolution of the Cu 3d-derived electronic states at or near E_F, as the long-range AFM-ordered insulator evolves into a metallic or superconducting state with decreasing the concentration of the Cu dopant in $NaFe_{1-x}Cu_xAs$.

In summary, using ARPES combined with DFT and DFT + U calculations, we have revealed the electronic structure of the heavily Cu-doped $NaFe_{1-x}Cu_xAs$ ($x = 0.44$) and showed that its ground state is a

narrow-gap insulator whose origin lies in strong electron interactions of Fe $3d$ orbitals. The on-site interaction (Hubbard U and Hund's coupling J_H) remove the hybridizations between Fe $3d$ and other Cu-As orbitals in the vicinity of E_F. The interactions furthermore elevate the Fe $3d$ bands near E_F to above the chemical potential and push the fully occupied Fe $3d$ valence band further down in binding energy. Consequently, an energy gap opens up about the chemical potential, instigating an insulating phase in the heavily Cu-doped $NaFe_{1-x}Cu_xAs$. The effect induced by U and J_H resembles the situation in the parent compounds of the high-T_c cuprates (Mott insulators), with the Mott induced charge-transfer gap that underscores the insulating behavior. The quantitative differences with cuprates are that the top of the valence band is derived from Cu-As hybridized bands and is very close to (or touching) the chemical potential, and the charge-transfer gap between valence and conduction bands is very narrow. The occupation of the Fe $3d$ conduction band by thermally activated electrons increases the hopping processes between the Fe sites and thus suppresses the AFM ordering, eventually destroying the long-range order at $T > T_N$.

We thank T. Schmitt, Zhiming Wang, and Bruce Normand for their help and enlightening discussions. This work was supported by the Swiss National Science Foundation (No. 200021-159678) and the Sino-Swiss Science and Technology Cooperation (Project No. IZLCZ2138954). The single crystal growth is supported by the U.S. DOE, BES, under Contract No. de-sc0012311, and by the National Natural Science Foundation of China Grant No. 51471135. The theoretical work at Rice was supported by the Robert A. Welch Foundation Grant No. C-1818 (A. H. N.) and by U.S. NSF Grant No. DMR-1350237 (A. H. N.).

*christian.matt@psi.ch
†ming.shi@psi.ch

[1] G. R. Stewart, Rev. Mod. Phys. **83**, 1589 (2011).
[2] J. Paglione and R. L. Greene, Nat. Phys. **6**, 645 (2010).
[3] Q. Si, R. Yu, and E. Abrahams, Nat. Rev. Mater. 16017 (2016).
[4] P. L. Bach, S. R. Saha, K. Kirshenbaum, J. Paglione, and R. L. Greene, Phys. Rev. B **83**, 212506 (2011).
[5] Z. P. Yin, K. Haule, and G. Kotliar, Nat. Mater. **10**, 932 (2011).
[6] M. R. Norman, D. Pines, and C. Kallin, Adv. Phys. **54**, 715 (2005).
[7] P. A. Lee, N. Nagaosa, and X.-G. Wen, Rev. Mod. Phys. **78**, 17 (2006).
[8] C. E. Matt, C. G. Fatuzzo, Y. Sassa, M. Månsson, S. Fatale, V. Bitetta, X. Shi, S. Pailhès, M. H. Berntsen, T. Kurosawa, M. Oda, N. Momono, O. J. Lipscombe, S. M. Hayden, J.-Q. Yan, J.-S. Zhou, J. B. Goodenough, S. Pyon, T. Takayama, H. Takagi*et al.*, Phys. Rev. B **92**, 134524 (2015).
[9] A. Georges, L. de'Medici, and J. Mravlje, Annu. Rev. Condens. Matter Phys. **4**, 137 (2013).
[10] L. de'Medici, G. Giovannetti, and M. Capone, Phys. Rev. Lett. **112**, 177001 (2014).
[11] N. Xu, P. Richard, A. van Roekeghem, P. Zhang, H. Miao, W.-L. Zhang, T. Qian, M. Ferrero, A. S. Sefat, S. Biermann, and H. Ding, Phys. Rev. X **3**, 011006 (2013).
[12] N. Xu, P. Richard, X.-P. Wang, X. Shi, A. van Roekeghem, T. Qian, E. Ieki, K. Nakayama, T. Sato, E. Rienks, S. Thirupathaiah, J. Xing, H.-H. Wen, M. Shi, T. Takahashi, and H. Ding, Phys. Rev. B **87**, 094513 (2013).
[13] D. Fang, X. Shi, Z. Du, P. Richard, H. Yang, X. X. Wu, P. Zhang, T. Qian, X. Ding, Z. Wang, T. K. Kim, M. Hoesch, A. Wang, X. Chen, J. Hu, H. Ding, and H.-H. Wen, Phys. Rev. B **92**, 144513 (2015).
[14] Y. Song, Z. Yamani, C. Cao, Y. Li, C. Zhang, J. Chen, Q. Huang, H. Wu, J. Tao, Y. Zhu, W. Tian, S. Chi, R. Yu, A. H. Nevidomskyy, E. Morosan, Q. Si, and P. Dai, arXiv: 1504.05116.
[15] A. F. Wang, J. J. Lin, P. Cheng, G. J. Ye, F. Chen, J. Q. Ma, X. F. Lu, B. Lei, X. G. Luo, and X. H. Chen, Phys. Rev. B **88**, 094516 (2013).
[16] S. Li, C. de la Cruz, Q. Huang, G. F. Chen, T.-L. Xia, J. L. Luo, N. L. Wang, and P. Dai, Phys. Rev. B **80**, 020504 (2009).
[17] E. Razzoli, M. Kobayashi, V. N. Strocov, B. Delley, Z. Bukowski, J. Karpinski, N. C. Plumb, M. Radovic, J. Chang, T. Schmitt, L. Patthey, J. Mesot, and M. Shi, Phys. Rev. Lett. **108**, 257005 (2012).
[18] V. Brouet, M. F. Jensen, P.-H. Lin, A. Taleb-Ibrahimi, P. Le Fèvre, F. Bertran, C.-H. Lin, W. Ku, A. Forget, and D. Colson, Phys. Rev. B **86**, 075123 (2012).
[19] K. Momma and F. Izumi, J. Appl. Crystallogr. **44**, 1272 (2011).
[20] U. Flechsig, L. Patthey, and T. Schmidt, AIP Conf. Proc. **705**, 316 (2004).
[21] P. Blaha, K. Schwarz, G. K. H. Madsen, D. Kvasnicka, and J. Luitz, *WIEN2K* (Vienna University of Technology, 2001).
[22] T. Miyake, K. Nakamura, R. Arita, and M. Imada, J. Phys. Soc. Jpn. **79**, 044705 (2010).
[23] See Supplemental Material, which includes Refs. [24–36], at http://link.aps.org/supplemental/10.1103/PhysRevLett.117.097001 for further information on our materials and methods.
[24] M. A. Tanatar, N. Spyrison, K. Cho, E. C. Blomberg, G. Tan, P. Dai, C. Zhang, and R. Prozorov, Phys. Rev. B **85**, 014510 (2012).
[25] J. P. Perdew, K. Burke, and M. Ernzerhof, Phys. Rev. Lett. **77**, 3865 (1996).
[26] V. I. Anisimov, I. V. Solovyev, M. A. Korotin, M. T. Czyżyk, and G. A. Sawatzky, Phys. Rev. B **48**, 16929 (1993).
[27] A. I. Liechtenstein, V. I. Anisimov, and J. Zaanen, Phys. Rev. B **52**, R5467 (1995).
[28] A. Charnukha, D. V. Evtushinsky, C. E. Matt, N. Xu, M. Shi, B. Büchner, N. D. Zhigadlo, B. Batlogg, and S. V. Borisenko, Sci. Rep. **5**, 18273 (2015).
[29] A. Charnukha, S. Thirupathaiah, V. B. Zabolotnyy, B. Büchner, N. D. Zhigadlo, B. Batlogg, A. N. Yaresko, and S. V. Borisenko, Sci. Rep. **5**, 10392 (2015).
[30] A. I. Coldea, J. D. Fletcher, A. Carrington, J. G. Analytis, A. F. Bangura, J.-H. Chu, A. S. Erickson, I. R. Fisher, N. E. Hussey, and R. D. McDonald, Phys. Rev. Lett. **101**, 216402 (2008).

[31] L. Ortenzi, E. Cappelluti, L. Benfatto, and L. Pietronero, Phys. Rev. Lett. **103**, 046404 (2009).
[32] M. Yi, D. H. Lu, J. G. Analytis, J.-H. Chu, S.-K. Mo, R.-H. He, R. G. Moore, X. J. Zhou, G. F. Chen, J. L. Luo, N. L. Wang, Z. Hussain, D. J. Singh, I. R. Fisher, and Z.-X. Shen, Phys. Rev. B **80**, 024515 (2009).
[33] L. de'Medici, Phys. Rev. B **83**, 205112 (2011).
[34] K. Haule and G. Kotliar, New J. Phys. **11**, 025021 (2009).
[35] J. E. Han, M. Jarrell, and D. L. Cox, Phys. Rev. B **58**, R4199 (1998).
[36] E. Razzoli, C. E. Matt, M. Kobayashi, X.-P. Wang, V. N. Strocov, A. van Roekeghem, S. Biermann, N. C. Plumb, M. Radovic, T. Schmitt, C. Capan, Z. Fisk, P. Richard, H. Ding, P. Aebi, J. Mesot, and M. Shi, Phys. Rev. B **91**, 214502 (2015).
[37] D. J. Singh, Phys. Rev. B **79**, 153102 (2009).
[38] S. F. Wu, P. Richard, A. van Roekeghem, S. M. Nie, H. Miao, N. Xu, T. Qian, B. Saparov, Z. Fang, S. Biermann, A. S. Sefat, and H. Ding, Phys. Rev. B **91**, 235109 (2015).
[39] C. Ye, W. Ruan, P. Cai, X. Li, A. Wang, X. Chen, and Y. Wang, Phys. Rev. X **5**, 021013 (2015).
[40] P. Richard, T. Sato, K. Nakayama, T. Takahashi, and H. Ding, Rep. Prog. Phys. **74**, 124512 (2011).
[41] N. Xu, P. Richard, X. Shi, A. van Roekeghem, T. Qian, E. Razzoli, E. Rienks, G.-F. Chen, E. Ieki, K. Nakayama, T. Sato, T. Takahashi, M. Shi, and H. Ding, Phys. Rev. B **88**, 220508 (2013).
[42] A. van Roekeghem, P. Richard, H. Ding, and S. Bierman, C.R. Phys. **17**, 140 (2016).
[43] P. W. Anderson, in *Solid State Physics*, edited by F. Seitz and D. Turnbull (Academic, New York, 1963), p. 99.
[44] P. W. Anderson, Rev. Mod. Phys. **50**, 191 (1978).
[45] S. Nakatsuji, D. Hall, L. Balicas, Z. Fisk, K. Sugahara, M. Yoshioka, and Y. Maeno, Phys. Rev. Lett. **90**, 137202 (2003).
[46] Y. Singh and P. Gegenwart, Phys. Rev. B **82**, 064412 (2010).
[47] J. E. Keem, J. M. Honig, and L. L. V. Zandt, Philos. Mag. B **37**, 537 (1978).
[48] D. E. McNally, J. W. Simonson, K. W. Post, Z. P. Yin, M. Pezzoli, G. J. Smith, V. Leyva, C. Marques, L. DeBeer-Schmitt, A. I. Kolesnikov, Y. Zhao, J. W. Lynn, D. N. Basov, G. Kotliar, and M. C. Aronson, Phys. Rev. B **90**, 180403 (2014).
[49] S.-I. Uchida, Jpn. J. Appl. Phys. **32**, 3784 (1993).
[50] M. Yi, D. H. Lu, R. Yu, S. C. Riggs, J.-H. Chu, B. Lv, Z. K. Liu, M. Lu, Y.-T. Cui, M. Hashimoto, S.-K. Mo, Z. Hussain, C. W. Chu, I. R. Fisher, Q. Si, and Z.-X. Shen, Phys. Rev. Lett. **110**, 067003 (2013).
[51] Y. Liu, D.-Y. Liu, J.-L. Wang, J. Sun, Y. Song, and L.-J. Zou, Phys. Rev. B **92**, 155146 (2015).
[52] S. T. Cui, S. Kong, S. L. Ju, P. Wu, A. F. Wang, X. G. Luo, X. H. Chen, G. B. Zhang, and Z. Sun, Phys. Rev. B **88**, 245112 (2013).